Quantum Nondemolition Detection of a Propagating Microwave Photon

Sankar R. Sathyamoorthy,[1] L. Tornberg,[1,*] Anton F. Kockum,[1] Ben Q. Baragiola,[2] Joshua Combes,[2] C. M. Wilson,[1,3] Thomas M. Stace,[4] and G. Johansson[1]

[1]*Department of Microtechnology and Nanoscience, MC2, Chalmers University of Technology, S-41296 Gothenburg, Sweden*
[2]*Center for Quantum Information and Control, University of New Mexico, Albuquerque, New Mexico 87131-0001, USA*
[3]*Institute for Quantum Computing and Electrical and Computer Engineering Department, University of Waterloo, Waterloo N2 L 3G1, Canada*
[4]*Centre for Engineered Quantum Systems, School of Physical Sciences, University of Queensland, Saint Lucia, Queensland 4072, Australia*

(Received 29 August 2013; revised manuscript received 19 December 2013; published 3 March 2014)

The ability to nondestructively detect the presence of a single, traveling photon has been a long-standing goal in optics, with applications in quantum information and measurement. Realizing such a detector is complicated by the fact that photon-photon interactions are typically very weak. At microwave frequencies, very strong *effective* photon-photon interactions in a waveguide have recently been demonstrated. Here we show how this type of interaction can be used to realize a quantum nondemolition measurement of a single propagating microwave photon. The scheme we propose uses a chain of solid-state three-level systems (transmons) cascaded through circulators which suppress photon backscattering. Our theoretical analysis shows that microwave-photon detection with fidelity around 90% can be realized with existing technologies.

DOI: 10.1103/PhysRevLett.112.093601 PACS numbers: 42.50.Dv, 42.50.Lc, 42.65.-k, 85.60.Gz

Quantum mechanics tells us that a measurement perturbs the state of a quantum system. In the most extreme case, this leads to the destruction of the measured quantum system. By coupling the system to a quantum probe, a quantum nondemolition [1] (QND) measurement can be realized, where the system is not destroyed by the measurement. Such a property is crucial for quantum error correction [2], state preparation by measurement [3,4], and one-way quantum computing [5]. For microwave frequencies, detection of confined photons in high-Q cavities has been proposed and experimentally demonstrated by several groups [6–9]. They all exploit the strong interaction between photons and atoms (real and artificial) on the single photon level. Detection schemes for traveling photons have also been suggested [10–12], but in those proposals the photon is absorbed by the detector and the measurement is therefore destructive. Proposals for detecting itinerant photons using coupled cavities have also been suggested, but they are limited by the trade-off between interaction strength and signal loss due to reflection [13]. Other schemes based on the interaction of Λ-type atomic level structures have been suggested, but the absence of such atomic level structures in solid-state systems make them unsuited to the microwave regime [14–16].

Here, we present a scheme to detect a propagating microwave photon in an open waveguide. At its heart is the strong *effective* nonlinear interaction between microwave fields induced by an artificial atom to which they are coupled. A single photon in the control field induces a detectable displacement in the state of a probe field, which is initially in a coherent state. The control field is not absorbed, making the protocol QND. The protocol may be operated either synchronously (in which the control photons arrive within specified temporal windows) or asynchronously [17].

Figure 1 illustrates the scheme. The effective nonlinear interaction between the control photon and the probe field is realized by N noninteracting artificial atoms (*transmon* devices [18]) coupled to the transmission line. Transmons are particularly attractive in light of recent work demonstrating strong atom-field coupling in the single-photon regime in open waveguides [19]. We treat the atoms as anharmonic three-level ladder systems with energy

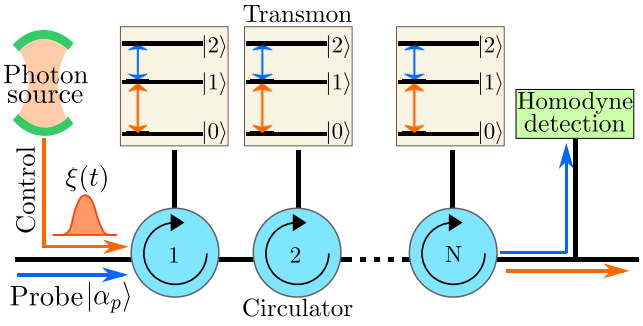

FIG. 1 (color online). A chain of N transmons cascaded from microwave circulators interacts with control and probe fields, which are close to resonance with the 0-1 and 1-2 transition, respectively. In the absence of a control photon, the chain is transparent to the probe. A control photon with temporal profile $\xi(t)$ drives each transmon consecutively, which then displaces the probe field, which is detected by homodyne measurement.

eigenstates $|0\rangle$, $|1\rangle$, and $|2\rangle$ designed such that the control and probe fields are close to resonance with the $|0\rangle \leftrightarrow |1\rangle$ and $|1\rangle \leftrightarrow |2\rangle$ transition, respectively. In the absence of a control photon, the system is completely transparent to the probe. A single control photon will sequentially excite the chain of transmons, displacing the state of the probe field [19], which we show can be detected by homodyne measurement of the probe.

While a single transmon in a waveguide induces a large photon-photon nonlinearity, the induced displacement of the probe field is nevertheless insufficient to yield a useful detection protocol [20]. Furthermore, Kramers-Kronig relations imply that there will be substantial backreflection of the control photon from a strongly coupled transmon, and it was shown that this precludes cascading additional transmons in an attempt to boost the probe displacement [20]. In order to evade this issue, we propose cascading transmons from stub waveguides attached to a chain of circulators, shown in Fig. 1. In this geometry, the circulators suppress backscattering [21] and the fields propagate unidirectionally along the waveguide. Thus, multiple transmons can interact with the control photon, which is fully transmitted to the output.

To provide a quantitative analysis of this proposal, we start by defining the transmon Hamiltonian ($\hbar = 1$)

$$H = -\omega_{01}|0\rangle\langle 0| + \omega_{12}|2\rangle\langle 2|. \tag{1}$$

We couple the transmons within a cascaded one-way channel which we treat using the input-output formalism [22–24]. The final output probe field of the chain yields information about the state of the control field, which we quantify through a suitably defined signal-to-noise ratio (SNR), and through a fidelity measure, F, the probability to infer the correct photon number in the control field.

We take two equivalent approaches to model the photon source [20]. In the first, we invoke a fictitious source cavity with resonance frequency ω_c and annihilation operator a to generate the control photon. In the rotating frame defined by the unitary transformation $U(t) = \exp\{it[\omega_c(|0\rangle\langle 0| + a^\dagger a) + \omega_p|2\rangle\langle 2|]\}$, where $\omega_{p/c}$ is the probe/control frequency, the dynamics of the cascaded system, including the control photon and backaction of the homodyne measurement, is given by the stochastic master equation (see Supplemental Material [25])

$$\begin{aligned} d\rho = &-i[H_{\text{eff}}, \rho]dt + \sqrt{\eta}\mathcal{M}[\Lambda_{12}]\rho dW(t) \\ &+ \left[\kappa\mathcal{D}[a] - \sqrt{\kappa}\mathcal{C}[a, \Lambda_{01}] + \sum_{j=1}^{N}\left(\mathcal{D}[L_{01}^{(j)}] + \mathcal{D}[L_{12}^{(j)}]\right.\right. \\ &\left.\left. - \sum_{k=j+1}^{N}\left(\mathcal{C}[L_{01}^{(j)}, L_{01}^{(k)}] + \mathcal{C}[L_{12}^{(j)}, L_{12}^{(k)}]\right)\right)\right]\rho dt, \end{aligned} \tag{2}$$

where $H_{\text{eff}} = \sum_{k=1}^{N} H^{(k)}$ is the effective Hamiltonian with the single transmon Hamiltonian given by $H^{(k)} = -\Delta_c^{(k)}|0\rangle\langle 0|^{(k)} + \Delta_p^{(k)}|2\rangle\langle 2|^{(k)} + \Omega_p(L_{12}^{(k)} + L_{21}^{(k)})$, $\Delta_c^{(k)} = \omega_{10}^{(k)} - \omega_c$ and $\Delta_p^{(k)} = \omega_{21}^{(k)} - \omega_p$ are the detunings between control and probe fields and the transition frequencies of transmon k, and Ω_p is the probe amplitude. We have defined $\mathcal{D}[c]\rho = c\rho c^\dagger - \frac{1}{2}c^\dagger c\rho - \frac{1}{2}\rho c^\dagger c$ [26], $L_{ij}^{(k)} = \sqrt{\Gamma_{ij}^{(k)}}|i\rangle\langle j|^{(k)}$, and $\Lambda_{ij} = \sum_{k=1}^{N} L_{ij}^{(k)}$, where $\Gamma_{ij}^{(k)} = \Gamma_{ji}^{(k)}$ are transmon decay rates. We allow different couplings between each transmon and the waveguide, which we numerically optimize to achieve high SNR. The cascaded, field-induced interaction between the transmons in the chain is described by the superoperator $\mathcal{C}[c_1, c_2]\rho = [c_2^\dagger, c_1\rho] + [\rho c_1^\dagger, c_2]$, and $\mathcal{M}[c]\rho = (e^{i\phi}c\rho + e^{-i\phi}\rho c^\dagger) - \langle e^{i\phi}c + e^{-i\phi}c^\dagger\rangle\rho$ is the measurement superoperator describing the backaction of the homodyne measurement with local oscillator phase ϕ and efficiency η [27]. $dW(t)$ is a Wiener increment satisfying $E[dW(t)] = 0$ and $E[dW(t)^2] = dt$. The control photon envelope $\xi(t)$ is set by the time-dependent cavity damping rate $\kappa(t) = \xi(t)/[\int_t^\infty |\xi(s)|^2 ds]^{1/2}$ [28]. Although the cavity considered here is notionally fictitious and serves merely as the photon source, we note that photon generation with cavities with or without tunable couplings have been demonstrated recently [29–31].

In the second approach, we adopt the Fock state master equation formalism, in which the control photon envelope appears explicitly [25,32]. In either of the approaches, the transmon dynamics are *not* adiabatically eliminated, but included explicitly (within the rotating wave approximation). Hence, we do not rely on any effective cross-Kerr-type Hamiltonian to mediate photon-photon interactions [16,33].

In either numerical simulations or an actual experimental implementation of this scheme, the stochastic output from the homodyne measurement of the probe field is $j_n(t)dt = \sqrt{\eta}\langle e^{i\phi}\Lambda_{12} + e^{-i\phi}\Lambda_{21}\rangle dt + dW(t)$, where n is the number of photons in the control field. The ultimate objective is to derive a signal S_n encoding the state of the control field from the homodyne current j_n. The most straightforward approach is to average j_n over a suitably optimized temporal window $S_n = \int_{t_i}^{t_f} j_n(t)dt$, where $t_m = t_f - t_i$ is the measurement window. In the absence of a control photon, j_n consists only of the quantum noise associated with the probe field, and so $E[S_0] = 0$, and the variance is $\text{var}[S_0] = t_m$. In the presence of a control photon, the probe field is displaced in phase space and the homodyne current acquires a time-dependent component [pictured in Fig. 2(c)], so $E[S_1] \neq 0$. Thus, we define the signal-to-noise ratio

$$\text{SNR} = E[S_1]/\sqrt{\text{var}[S_1] + t_m}. \tag{3}$$

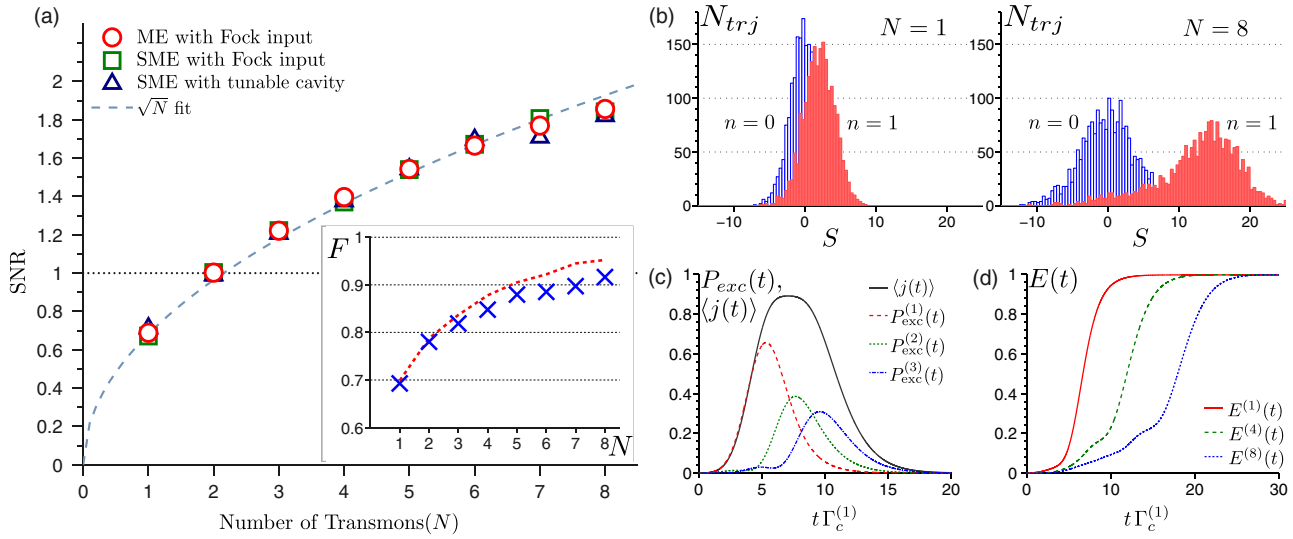

FIG. 2 (color online). Signal-to-noise ratio (SNR) and detector dynamics. (a) SNR calculated using the master equation (ME) with Fock state input (Supplemental Material [25]) (red circles), stochastic master equation (SME) with a Fock state input (green squares), and stochastic master equation with a tunable cavity as photon source (blue triangles). The dashed line shows a $\sqrt{N}$ fit assuming that each transmon contributes equally and independently to the signal. Inset: Detection fidelity F of correctly inferring the control photon number, Eq. (4). The crosses are results of Monte Carlo sampling from the stochastic master equation; the dashed line is inferred from the SNR, assuming a normal distribution. (b) Histogram of signal with 0 (blue) and 1 (red) control photons. For $N = 1$ transmon, the distributions overlap significantly (SNR = 0.7); for $N = 8$, the distributions are well resolved (SNR = 1.85). (c) Transmon excitation P_{exc} and average homodyne current $\langle j(t)\rangle$ over time for $N = 3$. (d) Integrated output photon flux for $N = 1$, 4, and 8, showing unity transmission. Transmon parameter values are listed in Table I, the homodyne local oscillator phase is $\phi = \pi/2$ and probe integration window $4 < t < 8 + 1.5(N - 1)$, a value which is found by numerical optimization to limit the amount of added noise to the signal. All quantities are in units of $\Gamma_c^{(1)} = \Gamma_{01}^{(1)}$.

We note that there are more optimal ways to define the signal S_n using linear or nonlinear filters on j_n [34]. We find that optimal linear filters improve the SNR modestly (Supplemental Material [25]), but for brevity and simplicity, the results in this Letter use the simple definitions above.

The mean of the homodyne current $\langle j(t)\rangle$ is given by the unconditional dynamics of Eq. (2). Using the quantum regression theorem, it is possible to calculate the variance from the unconditional dynamics, and one does not, in principle, need to solve the full stochastic evolution if interested in the signal-to-noise ratio as written above [35]. However, since the SNR does not contain any information about the signal distribution, a quantitative assessment of the measurement fidelity can only be done by Monte Carlo sampling the output of the full stochastic master equation of Eq. (2). We define the measurement fidelity, F, to be the probability of correctly inferring the state of the control field,

$$F = P(S < S_0^T|0)P(n = 0) + P(S > S_1^T|1)P(n = 1), \tag{4}$$

where $P(S \leq S_0^T|n)$ is the conditional probability that S is less than some predefined threshold S_n^T given the control field has n photons. For the purposes of this Letter, we assume the priors $P(0) = P(1) = 1/2$.

Figure 2(a) is the main quantitative result of this Letter, showing SNR as a function of the number of transmons N, assuming a Gaussian control-photon envelope $\xi(t)$ (see Table I). For a single transmon the SNR is around 0.7, consistent with the results in Ref. [20]. For $N = 2$ transmons, the SNR reaches unity and grows monotonically with N. Figure 2(b) shows the corresponding histograms of $S_{0,1}$ for $N = 1$ and $N = 8$. Clearly, the peaks are not resolved for $N = 1$, but they are well resolved for $N = 8$, consistent with improvement in SNR. For the latter, there is a notable skewness and increase in the width of the distribution for the one-photon case. Although this seems to indicate a slight memory effect, we can fit the SNR data in Fig. 2(a) to a simple $\sqrt{N}$ dependence, which is what we expect if each transmon contributed equally and independently to the signal. The crosses in the inset of Fig. 2(a) show the probability of correctly inferring the input photon number [using Eq. (4)] assuming a common threshold, $S_0^T = S_1^T$. The dashed line is a theoretical fit estimated from the SNR assuming Gaussian distributions, which slightly overestimates the fidelity, on account of the non-Gaussian skewness in the histograms.

If a definitive measurement result is not required, the value of F can be improved by choosing separate thresholds, $S_0^T < S_1^T$, such that the data falling between the thresholds are rejected as inconclusive. Our analysis shows

TABLE I. Parameter values for which the SNR is plotted in Figs. 2 and 3. All of the rates are in units of $\Gamma_c^{(1)}$. The values of other parameters are $\Gamma_p^i = 2\Gamma_c^i$, $\Delta_c^i = 0$, $\Delta_p^i = 0$. 2000 trajectories are used in the simulation for each control input state.

Photon shape	$\xi(t)$	Γ_{ph}	T_{ph}	$\Gamma_c^{(1)}$	$\Gamma_c^{(2)}$	$\Gamma_c^{(3)}$	$\Gamma_c^{(4)}$	$\Gamma_c^{(5)}$	$\Gamma_c^{(6)}$	$\Gamma_c^{(7)}$	$\Gamma_c^{(8)}$	Ω_p^2	χ
Gaussian	$[\Gamma_{ph}^2/(2\pi)]^{1/4}\exp[-\Gamma_{ph}^2(t-T_{ph})^2/4]$	0.8	4	1.0	1.9	2.2	2.5	2.4	2.5	2.7	3.2	0.12	0.6813
Decaying exponential	$\Theta(T_{ph}-t)\sqrt{\Gamma_{ph}}\exp(-\Gamma_{ph}t/2)$	0.5	4	1.0	1.6	2.1	2.5	2.6	2.9	3.5	3.8	0.16	0.5272
Rising exponential	$\Theta(t-T_{ph})\sqrt{\Gamma_{ph}}\exp(\Gamma_{ph}t/2)$	0.5	12	1.0	1.9	2.3	2.6	3.0	3.3	3.5	3.8	0.16	0.5424

that with eight transmons a value of $F = 0.95$ ($F = 0.90$) can be reached with 15% (0%) of the measurement records being rejected. These numbers are above or comparable to the measurement efficiencies quoted in Refs. [10–12], and we stress the fact that the detection schemes proposed there were destructive.

The detector dynamics is shown in Fig. 2(c), showing the excitation probability of each transmon as function of time for $N = 3$ along with the average homodyne signal $\langle j(t)\rangle$. As the excitation is relayed through the chain, each transmon contributes to S, overwhelming the quantum noise in the probe. The results in Fig. 2 were obtained for an optimized set of parameter values by numerically tuning Δ_c, Δ_p, $\Gamma_c = \Gamma_{01}$, and $\Gamma_p = \Gamma_{12}$ independently for each transmon. We emphasize that this is quite robust: we can get SNR > 1 for a wide range of parameters (Supplemental Material [25]). Figure 2(d) shows the integrated control photon flux (Supplemental Material [25]), which

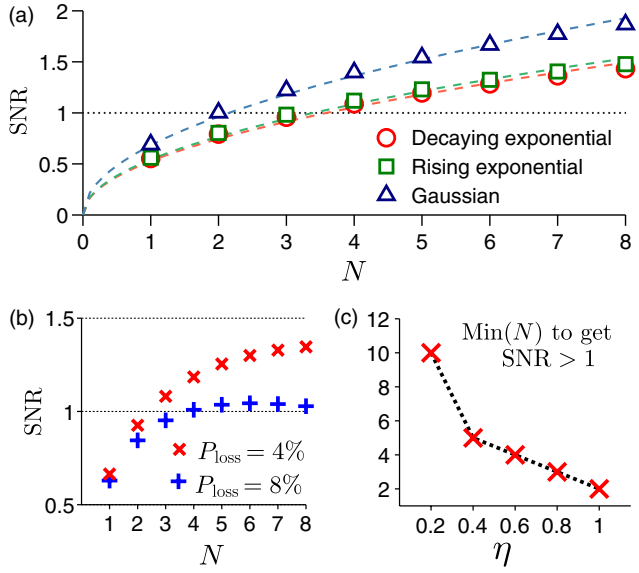

FIG. 3 (color online). (a) SNR with different input photon shapes. The parameters of the transmons and the probe field are optimized for each of the pulse shapes (see Table I). The dashed lines are fitted using $\chi\sqrt{N}$; the best-fit values of χ are in Table I. (b) Effect of losses in circulators on the SNR for a Gaussian input photon for two realistic choices of power loss $P_{\rm loss}$ in each circulator. (c) Number of transmons that would be required to achieve SNR ≥ 1 for a Gaussian input photon for detector efficiency η.

asymptotes to unity, indicating that the detector is transparent to the control field, making the protocol QND, albeit with some distortion in the control photon envelope. At the expense of a slightly diminished fidelity, F, we can choose the transmon coupling strengths to preserve the control photon envelope (Supplemental Material [25]). Figure 3(a) shows the SNR for non-Gaussian control-photon envelopes, $\xi(t)$, which are quantitatively somewhat worse than the Gaussian case, but not qualitatively so.

Circulators underpin the operation of this proposal. In practice, commercial circulators suffer both insertion loss and limited isolation. Both of these effects can be modeled as losses appearing at the input to the circulator: insertion loss is obvious, while imperfect isolation manifests as backscattering or nonefficient interaction, which we treat as a loss process (Supplemental Material [25]). We simulate both of these imperfections by interleaving fictitious beam splitters at the input to each circulator (Supplemental Material [25]). Figure 3(b) shows the SNR as a function of N for 4% and 8% power loss . Since more power is lost with larger N, we see that the previously monotonically increasing SNR now acquires a maximum value. Importantly, we see that it is still possible to get SNR ≥ 1 with realistic numbers (5%–10%) [36], and we expect this to be an even smaller issue if on-chip circulators [37] are realized.

Figure 3(c) shows the performance of the proposed detector when the efficiency of homodyne detection is less than 100%. Reassuringly, the overhead caused by an inefficient detector is not too high. With current state-of-the-art amplifiers [38], this scheme should be able to detect photons with a moderate number of transmons. The proposal is not impacted significantly by dephasing (Supplemental Material [25]).

In principle, the probe beam can be left on, since the detector is transparent to the probe when no control photons are present. In our analysis we assume that the *a priori* probability of a photon in a given temporal window is 50%. This is consistent with applications where the possible arrival time of the photon is known *a priori*. However, the detector may be operated in an asynchronous running mode (in which the *a priori* control photon probability in a given temporal window is not 50%), where the integration window of temporal width t_m slides over the entire duration of the homodyne measurement, and photon arrivals will be marked by a peak in this moving average.

In conclusion, we have proposed and analyzed a microwave photon detector consisting of a chain of transmon qubits. We show that a modest number of transmons connected by circulators is enough to achieve SNR ≥ 1 and a measurement fidelity $> 90\%$. We anticipate that analogous protocols could be used to detect other itinerant bosonic particles, e.g., phonons [39], and, together with postselection, be used for probabilistic generation of nonclassical states of the bosonic field.

We thank Per Delsing, Bixuan Fan, Io Chun Hoi, and Gerard Milburn for fruitful discussions. We acknowledge financial support from the Swedish Research Council, the Wallenberg Foundation, STINT, and the EU through the projects SOLID and PROMISCE. T. M. S. is funded by the ARC Research Fellowship program and the ARC Centre of Excellence in Engineered Quantum Systems. B. Q. B. and J. C. acknowledge support from NSF Grants No. PHY-1212445 and No. PHY-1005540, AFOSR Grant No. Y600242, and ONR Grant No. N00014-11-1-0082.

*lars.tornberg@chalmers.se

[1] V. Braginski and F. Khalili, *Quantum Measurements* (Cambridge University Press, Cambridge, England, 1992).
[2] A. M. Steane, Phys. Rev. Lett. **77**, 793 (1996).
[3] R. Ruskov and A. N. Korotkov, Phys. Rev. B **67**, 241305 (2003).
[4] L. S. Bishop, L. Tornberg, D. Price, E. Ginossar, A. Nunnenkamp, A. A. Houck, J. M. Gambetta, J. Koch, G. Johansson, S. M. Girvin, and R. J. Schoelkopf, New J. Phys. **11**, 073040 (2009).
[5] R. Raussendorf and H. J. Briegel, Phys. Rev. Lett. **86**, 5188 (2001).
[6] D. I. Schuster, A. A. Houck, J. A. Schreier, A. Wallraff, J. M. Gambetta, A. Blais, L. Frunzio, J. Majer, B. Johnson, M. H. Devoret, S. M. Girvin, and R. J. Schoelkopf, Nature (London) **445**, 515 (2007).
[7] C. Guerlin, J. Bernu, S. Deléglise, C. Sayrin, S. Gleyzes, S. Kuhr, M. Brune, J. Raimond, and S. Haroche, Nature (London) **448**, 889 (2007).
[8] H. Wang, M. Hofheinz, M. Ansmann, R. C. Bialczak, E. Lucero, M. Neeley, A. D. O'Connell, D. Sank, J. Wenner, A. N. Cleland, and J. M. Martinis, Phys. Rev. Lett. **101**, 240401 (2008).
[9] B. R. Johnson, M. D. Reed, A. A. Houck, D. I. Schuster, L. S. Bishop, E. Ginossar, J. M. Gambetta, L. DiCarlo, L. Frunzio, S. M. Girvin, and R. J. Schoelkopf, Nat. Phys. **6**, 663 (2010).
[10] G. Romero, J. J. Garcia-Ripoll, and E. Solano, Phys. Rev. Lett. **102**, 173602 (2009).
[11] Y.-F. Chen, D. Hover, S. Sendelbach, L. Maurer, S. T. Merkel, E. J. Pritchett, F. K. Wilhelm, and R. McDermott, Phys. Rev. Lett. **107**, 217401 (2011).
[12] B. Peropadre, G. Romero, G. Johansson, C. M. Wilson, E. Solano, and J. J. Garcia-Ripoll, Phys. Rev. A **84**, 063834 (2011).
[13] F. Helmer, M. Mariantoni, E. Solano, and F. Marquardt, Phys. Rev. A **79**, 052115 (2009).
[14] D. Witthaut, M. D. Lukin, and A. S. Sørensen, Europhys. Lett. **97**, 50007 (2012).
[15] A. D. Greentree, R. G. Beausoleil, L. C. L. Hollenberg, W. J. Munro, Kae Nemoto, S. Prawer, and T. P. Spiller, New J. Phys. **11** 093005 (2009).
[16] W. J. Munro, K. Nemoto, R. G. Beausoleil, and T. P. Spiller, Phys. Rev. A **71**, 033819 (2005).
[17] A. Reiserer, S. Ritter, and G. Rempe, Science **342**, 1349 (2013).
[18] J. Koch, T. M. Yu, J. Gambetta, A. A. Houck, D. I. Schuster, J. Majer, A. Blais, M. H. Devoret, S. M. Girvin, and R. J. Schoelkopf, Phys. Rev. A **76**, 042319 (2007).
[19] I. C. Hoi, A. F. Kockum, T. Palomaki, T. M. Stace, B. Fan, L. Tornberg, S. R. Sathyamoorthy, G. Johansson, P. Delsing, and C. M. Wilson, Phys. Rev. Lett. **111** 053601 (2013).
[20] B. Fan, A. F. Kockum, J. Combes, G. Johansson, I. C. Hoi, C. M. Wilson, P. Delsing, G. J. Milburn, and T. M. Stace, Phys. Rev. Lett. **110**, 053601 (2013).
[21] K. Stannigel, P. Rabl, and P. Zoller, New J. Phys. **14**, 063014 (2012).
[22] H. J. Carmichael, Phys. Rev. Lett. **70**, 2273 (1993).
[23] C. W. Gardiner, Phys. Rev. Lett. **70**, 2269 (1993).
[24] J. Gough and M. R. James, Commun. Math. Phys. **287**, 1109 (2009).
[25] See Supplemental Material at http://link.aps.org/supplemental/10.1103/PhysRevLett.112.093601 for the derivation of master equations and a more detailed robustness analysis.
[26] G. Lindblad, Commun. Math. Phys. **48**, 119 (1976).
[27] H. M. Wiseman and G. J. Milburn, Phys. Rev. A **47**, 642 (1993).
[28] J. E. Gough, M. R. James, H. I. Nurdin, and J. Combes, Phys. Rev. A **86**, 043819 (2012).
[29] Y. Yin, Y. Chen, D. Sank, P. J. J. O'Malley, T. C. White, R. Barends, J. Kelly, E. Lucero, M. Mariantoni, A. Megrant, C. Neill, A. Vainsencher, J. Wenner, A. N. Korotkov, A. N. Cleland, and J. M. Martinis, Phys. Rev. Lett. **110**, 107001 (2013).
[30] C. Lang, C. Eichler, L. Steffen, J. M. Fink, M. J. Wooley, A. Blais, and A. Wallraff, Nat. Phys. **9**, 345 (2013).
[31] M. Pechal, C. Eichler, S. Zeytinoglu, S. Berger, A. Wallraff, and S. Filipp, arXiv:1308.4094.
[32] B. Q. Baragiola, R. L. Cook, A. M. Brańczyk, and J. Combes, Phys. Rev. A **86**, 013811 (2012).
[33] N. Imoto, H. A. Haus, and Y. Yamamoto, Phys. Rev. A **32**, 2287 (1985).
[34] J. Gambetta, W. A. Braff, A. Wallraff, S. M. Girvin, and R. J. Schoelkopf, Phys. Rev. A **76**, 012325 (2007).
[35] H. M. Wiseman and G. J. Milburn, *Quantum Measurement and Control* (Cambridge University Press, Cambridge, England, 2010).
[36] See data sheets for commercial circulators available at, e.g., http://pamtechinc.com or http://www.raditek.com.
[37] J. Koch, A. A. Houck, K. L. Hur, and S. M. Girvin, Phys. Rev. A **82**, 043811 (2010).
[38] F. Mallet, M. A. Castellanos-Beltran, H. S. Ku, S. Glancy, E. Knill, K. D. Irwin, G. C. Hilton, L. R. Vale, and K. W. Lehnert, Phys. Rev. Lett. **106**, 220502 (2011).
[39] M. Gustafsson, P. V. Santos, G. Johansson, and P. Delsing, Nat. Phys. **8**, 338 (2012).